Flow Beneath a Ship at Small Underkeel Clearance

Tim Gourlay

Centre for Marine Science and Technology, Curtin University of Technology, Western Australia

This article looks at the case of a large, flat-bottomed ship, such as a bulk carrier, moving in close proximity to a flat sea floor. It is shown that the flow beneath the ship can be modeled as a shear flow between two parallel plates, one of which is moving. The resulting flow can be represented using laminar Couette flow at low Reynolds numbers (possible at model scale) or the very different turbulent Couette flow at high Reynolds numbers (full scale). Implications of these flow models on squat and viscous resistance are discussed.

1. Introduction

MUCH THEORETICAL RESEARCH has been done into the flow around a ship operating in shallow water, using Prandtl's (1904) thin-boundary-layer theory to neglect the effect of viscosity in finding pressures around the hull. Tuck (1966) developed a shallow-water theory for slender hulls, which he used to find the leading order squat and wave resistance of a ship traveling in calm water, in the case where the water depth is small compared to the ship length. Similar methods were applied to seakeeping in shallow water in Beck and Tuck (1972), in the case where the depth is small compared to the incident wavelength.

More recently, slender-body methods including the effect of dispersion have been applied to ships moving in open water (Mei 1976, Gourlay & Tuck 2001). Methods involving dispersion and nonlinearity have been applied to ships in channels (Chen & Sharma 1995).

All the above methods have no explicit dependence on underkeel clearance, with the hull's waterline beam and section area at each station, as well as the water depth, being the primary input quantities. According to slender-body theory, the actual shape of each underwater section, and its proximity to the sea floor, is of secondary importance. For example, there is no problem in the theories with having a section area that is greater than the waterline beam times the water depth.

This simple treatment of the problem is made possible through the slender-body and shallow-water assumptions, as well as the application of Prandtl's theory.

However, the validity of neglecting viscosity becomes not altogether clear when a ship is operating at a very small underkeel clearance. In this case the ability of the outer flow to remain essentially inviscid is severely restricted beneath the hull by the no-slip condition on the sea floor.

In this paper we shall be looking at the modified flow that occurs when a large, flat-bottomed ship (such as a tanker or bulk carrier) is moving in close proximity to a rigid, flat sea floor.

2. Free hull boundary layer

We will consider a frame of reference in which the ship is fixed and the water is streaming past it. For a large, flat-bottomed ship traveling in water such that the underkeel clearance is not small, the boundary layer on the ship's hull grows in thickness from the bow toward the stern, as shown in Fig. 1.

The general character of the boundary layer may be estimated based on flat plate boundary layer theory. As an example case, which we shall use throughout this article, let us consider a 300 m L_{PP} MarAd L-Series bulk carrier (Roseman 1987) traveling at 10 knots in shallow water. The keel line of this vessel is parallel over almost its entire length, and the parallel midbody (from station 9 to 17, station 20 = FP) has a flat bottom with width slightly less than the ship's beam.

For a smooth flat plate, transition to turbulence is observed to occur at a local Reynolds number $\mathrm{Re}_x \approx 5 \times 10^5$ (see, e.g., White 1999, p. 439), where:

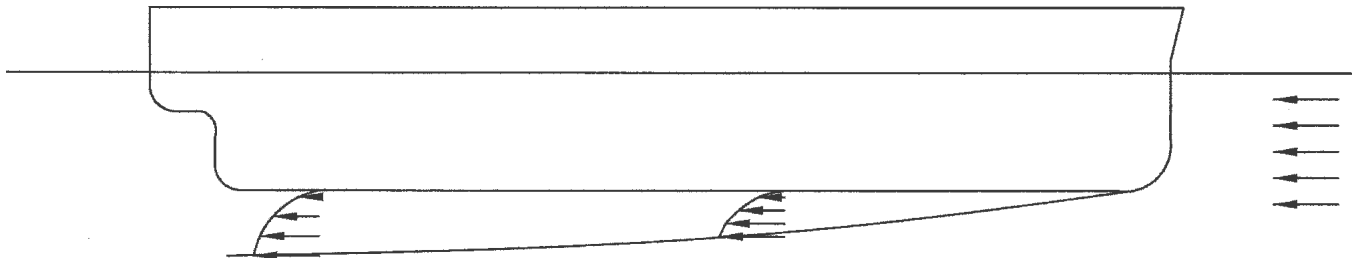$\mathrm{Re}_x = Vx/v$

   V = flow speed past the plate (approximately equal to the speed of the ship in this case, i.e., 10 knots)

   x = distance from the leading edge (distance from the bow in this case)

   v = kinematic viscosity of the fluid (we will consider salt water at 20 deg C, for which $v = 1.04 \times 10^{-6}$ m^2/s).

Fig. 1 Free boundary layer beneath a vessel at moderate or large underkeel clearance

Solving gives $x \approx 0.1$ m. Although the exact transition point will be delayed by the favorable pressure gradient near the bow, it is clear that the boundary layer will be almost entirely turbulent.

For a turbulent boundary layer past a flat plate, the boundary layer thickness δ grows downstream from the leading edge according to the approximate empirical relation (White 1999, p. 428):

$$\delta \approx \frac{0.16x}{\mathrm{Re}_x^{1/7}} \qquad (1)$$

Solving with $x = 300$ m gives $\delta = 2.3$ m. Therefore, near the vessel's stern the boundary layer thickness is expected to be around 2 to 2.5 m beneath the hull.

3. Interaction of the hull boundary layer with the sea floor

3.1. Possible flow patterns

Now let us consider how the free boundary layer, described above, will be affected when the ship is traveling with an underkeel clearance significantly less than the 2 m free boundary layer thickness described above.

Clearly, the boundary layer cannot exist in its unrestricted form over the length of the hull in this case. The no-slip condition on the sea floor means that in the ship-fixed frame of reference, the flow is required to move at exactly the speed of the free stream on the sea floor. This severely restricts the ability of the boundary layer to develop and will cause a very different type of flow between the hull and sea floor.

Except near the turn of the bilge, transverse pressure gradients will be small beneath the hull. The no-slip conditions on the hull

and sea floor will dominate the flow, causing flow to be almost purely longitudinal beneath the hull.
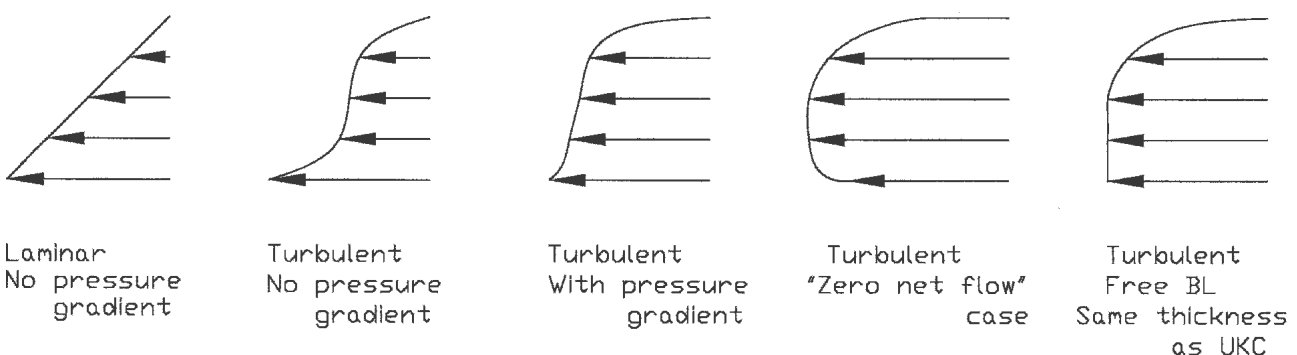
Near the bow, the flow is expected to be similar to the large-UKC case, as the boundary layer starts to grow along the hull. Apart from the moving wall, this flow has similarities with an entrance flow in a pipe, where the wall boundary layers grow and then merge to give a fully developed flow. In that case (White 1999), the entrance length is around 30 to 40 times the pipe diameter at the Reynolds numbers that we are dealing with (order 10^6 based on the transverse dimension). In the entrance region, the inviscid core is accelerated to preserve continuity, with a large pressure gradient required.

For flow beneath a ship, however, the flow is not an internal flow, meaning that much less longitudinal pressure gradient is present. Essentially, much of the flow is diverted around the sides of the ship rather than being forced beneath it. Therefore, the flow beneath the ship is governed mainly by the no-slip conditions on the hull and sea floor and may become fully developed more quickly than for the equivalent pipe flow.

Once the flow is fully developed, continuity requires that the velocity distribution be almost uniform over the whole area beneath the flat bottom of the ship. Therefore, unlike a free boundary layer, which grows steadily toward the stern, we would expect the velocity distribution to be almost uniform beneath the ship when the underkeel clearance is small.

An insight into the possible flow patterns in this case can be obtained from experimental results for flow between two parallel plates, one of which is moving. This flow is termed Couette flow (see, e.g., Schlichting 1968) and is a well-studied problem for either laminar or turbulent flow, with or without longitudinal pressure gradient.

A comparison of the mean velocity profiles for each type of Couette flow is shown in Fig. 2. At low Reynolds numbers, the

Laminar
No pressure gradient

Turbulent
No pressure gradient

Turbulent
With pressure gradient

Turbulent
"Zero net flow" case

Turbulent
Free BL
Same thickness as UKC

Fig. 2 Comparison of mean velocity profiles for Couette flow between two plates

flow is laminar and follows a linear velocity profile in the absence of a longitudinal pressure gradient. The presence of a pressure gradient superimposes a parabolic velocity profile onto the linear shear flow (Schlichting 1968).

For high Reynolds numbers, the flow is turbulent, and in the absence of a pressure gradient, an antisymmetric S-shaped velocity profile results (Reichardt 1956). A longitudinal pressure gradient causes the velocity profile to bulge out in the direction of decreasing pressure (Lund & Bush 1980).

Since the free turbulent boundary layer cannot grow indefinitely along the ship's hull because of the presence of the sea floor, it is expected that the flow will instead resemble a Couette flow between the hull and sea floor.

3.2. Laminar or turbulent flow?

Reichardt (1956) conducted a series of experiments on shear flows between two parallel plates with no longitudinal pressure gradient. It was found that the existence of turbulence was dependent on a Reynolds number

$$\text{Re}_H = \frac{VH}{\nu}$$

where

V = relative speed between plates
H = distance between plates.

Reichardt found that such shear flows tended to become turbulent and hence stray from a linear velocity profile, when $\text{Re}_H > 3{,}000$. Note that Reichardt's (1956) results and Schlichting's (1968) reproductions are quoted in terms of U, the speed of each plate with respect to the still midplane, that is, half of V. We shall instead use V for consistency.

For our example ship traveling at 10 knots, this Reynolds number is $\text{Re}_H = 5 \times 10^6$ with 1 m of clearance in the squatted position. The shear flow is indeed turbulent and will be at any realistic underkeel clearance.

Note that at model scale, the shear flow beneath the hull may still be laminar. For example, a 1:150 scale model of this example hull, traveling at the same depth Froude number and relative clearance, would have a Reynolds number $\text{Re}_H = 3 \times 10^3$, so that the shear flow is almost laminar. Also, any artificially generated turbulence (e.g., by turbulence studs) may be damped quite quickly by the small clearance between the hull and tank floor.

3.3. Effect of longitudinal pressure gradient

In the absence of any longitudinal pressure gradient, the turbulent Couette flow beneath a ship will be antisymmetric (see Fig. 2), with the mean flow speed equal to half the ship speed, that is, $V/2$.

For the mean flow speed to be greater than $V/2$, a pressure difference must be maintained between the bow and stern of the ship. This is feasible, since there is a high-pressure stagnation area near the ship's bow and low-pressure separated flow area near the stern. Inflow into the propeller also has the effect of decreasing the pressure ahead of the propeller, adding to the overall longitudinal pressure gradient.

An insight into the importance of longitudinal pressure gradient on the flow may be obtained by estimating the pressure drop over the ship's length, for the case where the mean flow speed beneath the ship is equal to the upstream flow speed V. This means that there is zero net flow relative to the sea floor. This "zero net flow" case (also shown in Fig. 2) was studied theoretically by Lund and Bush (1980), with reference to the experimental results of Huey and Williamson (1974).

Results were given up to $\text{Re}_H = 1 \times 10^5$ for smooth plates, and at this value it was found both theoretically and experimentally that the magnitude of the longitudinal pressure gradient was given by

$$\left| \frac{dp}{dx} \right| = 0.0032 \frac{\rho V^2}{2H} \tag{2}$$

This can be compared to the pressure drop for turbulent flow in a pipe, with the plate separation H likened to the pipe diameter d. The Darcy friction factor (see, e.g., White 1999) is 0.0032 for the Couette zero net flow case. For a smooth-walled circular pipe at $\text{Re}_d = 1 \times 10^5$, the Moody chart (see, e.g., White 1999) gives a Darcy friction factor of 0.018, around six times larger than the Couette zero-net flow case.

For comparison, Lund and Bush (1980) also give results for Poiseuille flow between two plates (flow between two stationary plates under a longitudinal pressure gradient). At $\text{Re}_H = 1 \times 10^4$ (based on mean flow speed V), the Darcy friction factor is 0.007, compared to 0.030 for a smooth-walled pipe at this Reynolds number. Therefore, the Darcy friction factor for a pipe is around four times larger than for flow between two plates. The pressure drop for zero net flow Couette flow is smaller than for Poiseuille flow, since in the former case one wall is moving at the same speed as the mean flow.

Equation (2) is valid for $\text{Re}_H = 1 \times 10^5$, which was the upper limit of Reynolds numbers calculated in Lund and Bush (1980) or obtained experimentally in Huey and Williamson (1974). An estimate of the pressure drop at $\text{Re}_H = 5 \times 10^6$ may be obtained by assuming a similar drop in Darcy friction factor as would occur for flow in a pipe with this Reynolds number change (50% decrease from $\text{Re}_H = 1 \times 10^5$ to 5×10^6). This gives a longitudinal pressure gradient of 2×10^1 Pa/m, which requires a pressure differential of 6 kPa between the bow and stern of a 300 m vessel traveling at 10 knots.

This required pressure differential is significant when compared to the stagnation pressure (above hydrostatic) of $\frac{1}{2}\rho V^2 = 13.5$ kPa in this case. Such a large pressure at the bow would not be achieved if the mean flow speed beneath the hull was close to the free stream speed.

However, the pressure drop between the bow and stern will be significant enough that the flow will not follow the antisymmetric velocity profile that occurs with zero pressure gradient.

Instead, the actual flow will be somewhere between these two scenarios: a turbulent Couette flow with pressure gradient, as indicated in Fig. 3. The mean flow speed beneath the hull will be such that the pressure rise at the bow (due to decrease in flow speed) is sufficient to provide the longitudinal pressure gradient required to drive the flow between the hull and sea floor at this mean flow speed. As stated previously, continuity requires that this velocity distribution be taken up close to the ship's bow and remain approximately uniform over the whole area beneath the flat bottom of the ship.
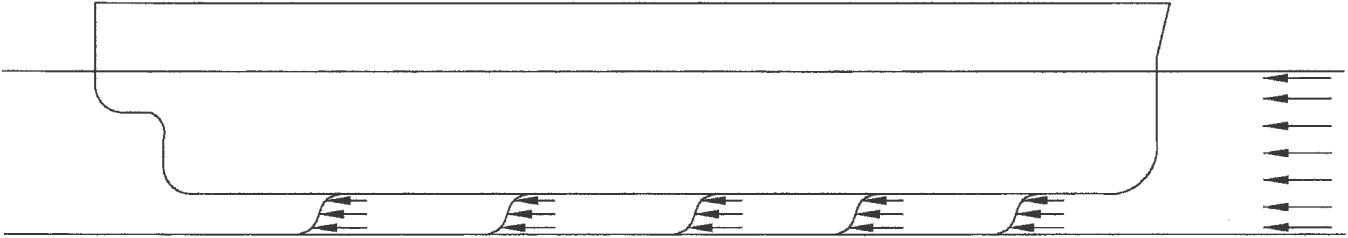
Fig. 3 Suggested model for flow beneath a ship at small underkeel clearance

Because of the decreased flow beneath the ship, more water will be diverted around the sides of the ship, further reinforcing the notion of almost-horizontal flow around a ship in shallow water (Tuck 1966).

4. Effect of small underkeel clearance on viscous resistance

Schlichting (1934) conducted an investigation into the effect of shallow water on ship resistance. This article is well summarized in Harvald (1983). Schlichting concluded that, at subcritical speeds, both the wave-making and frictional resistance of a hull tend to increase as the water depth decreases. The increase in wave-making resistance due to the changed wave pattern in shallow water is a well-known phenomenon. The increase in frictional resistance is a more subtle effect; Schlichting (1934) suggested that this is principally due to the two-dimensional nature of the flow in shallow water, causing larger flow velocities past the hull than in deep water. An empirical method was suggested for estimating the likely proportional increase in both wave making and frictional resistance of a general hull, based on results from model tests.

Schlichting's method, like the slender-body methods described in the Introduction, uses the hull section area and water depth to define the resistance changes. Therefore, resistance increase is judged to be primarily a shallow-water flow effect, rather than a small-underkeel clearance effect, and has no explicit dependence on underkeel clearance. Two hulls of the same section area but differing beams and drafts are expected to have similar frictional resistance.

However, what happens when the underkeel clearance becomes sufficiently small that the normal assumption of an unperturbed boundary layer over the hull surface is violated? Will the frictional drag on the bottom of the hull increase or decrease when the ship is moving in close proximity to the sea floor?

For the purposes of this simple discussion, we shall again model the region between the flat bottom of the ship and the flat sea floor as the flow between two parallel plates, one of which is moving.

For comparison, we shall first calculate the drag of a free boundary layer, representing the case when the ship's underkeel clearance is not small.

4.1. Free boundary layer

An empirical formulation for the wall shear stress τ_0 due to an unrestricted turbulent boundary layer flowing past a smooth flat plate is (see, e.g., White 1999, p. 442)

$$\tau_0 \approx \rho U^2 \frac{0.014}{\mathrm{Re}_x^{1/7}} \qquad (3)$$

where Re_x is the Reynolds number based on distance x from the leading edge. Unlike a laminar boundary layer, where the shear stress is significantly larger near the leading edge than further downstream, turbulent shear stress is only weakly dependent on distance from the leading edge. Nevertheless, it is still largest near the leading edge.

Integrating the shear stress over the area A of the plate yields the friction drag D on the plate. The nondimensional drag coefficient c_D then becomes (see, e.g., White 1999. p. 442)

$$c_D = \frac{D}{\frac{1}{2}\rho U^2 A} \approx \frac{0.031}{\mathrm{Re}_L^{1/7}} \qquad (4)$$

Here Re_L is the Reynolds number based on total plate length from the leading edge to the trailing edge. With $L = 300$ ms, $V = 10$ knots, and $\nu = 1.04 \times 10^{-6}$ m²/s; this gives a friction drag coefficient $c_D = 0.0015$.

4.2. Couette flow: zero pressure gradient

For turbulent shear flow between two flat plates, Reichardt (1956) determined experimentally that the velocity distribution near each plate follows the same standard logarithmic law as turbulent boundary layers or turbulent pipe flow (see, e.g., Schlichting 1968). The flow is antisymmetric about the mid-plane between the two plates, as depicted in Fig. 2. Near the stationary plate, the flow speed u at distance y from the plate satisfies the dimensionless equation

$$\frac{u}{u^*} = \frac{1}{\kappa} \ln\left(\frac{u^* y}{\nu}\right) + B \qquad (5)$$

where

$$u^* = \sqrt{\frac{\tau_0}{\rho}} = \text{"friction velocity"}$$

τ_0 = wall shear stress
κ = empirically determined constant, ≈ 0.41
B = empirically determined constant, ≈ 5.0 (depending on wall roughness).

For shear flow between two plates with zero pressure gradient, the shear stress is constant everywhere between the plates, and equal to its value at the wall τ_0 (Schlichting 1968).

The friction velocity $u*$ can be written in terms of the friction coefficient c_f, since

$$c_f = \frac{\tau_0}{\frac{1}{2}\rho V^2} = \frac{(u*)^2}{\frac{1}{2}V^2} \Rightarrow u* = V\sqrt{\frac{c_f}{2}}$$

Equation (5) can therefore be written

$$\frac{u}{V}\sqrt{\frac{2}{c_f}} = \frac{1}{\kappa}\ln\left(\sqrt{\frac{c_f}{2}}\,\mathrm{Re}_H\frac{y}{H}\right) + B \qquad (6)$$

Note that equation (6) is not valid exactly at the wall, since $u \to -\infty$ as $y \to 0$ according to this equation, when in fact $u = 0$ when $y = 0$.

For a turbulent shear flow with no longitudinal pressure gradient, the velocity distribution and shear stress can be calculated, using the fact that midway between the plates the flow speed must be half the relative velocity between the plates (by symmetry). Putting $u = V/2$ at $y = H/2$ in equation (6) gives

$$\frac{1}{\sqrt{2c_f}} = \frac{1}{\kappa}\ln\left(\frac{\sqrt{2c_f}}{4}\,\mathrm{Re}_H\right) + B \qquad (7)$$

This can be solved for c_f as a function of Re_H.

For example, using a plate separation (corresponding to underkeel clearance) of $H = 1.0$ ms, and plate relative velocity (corresponding to ship speed) of $V = 10$ knots, the Reynolds number is

$$\mathrm{Re}_H = 5 \times 10^6$$

and the friction coefficient is

$$c_f = 0.00051$$

if the effect of longitudinal pressure gradient is neglected.

Since this friction coefficient is constant over the length of the plate for which the turbulent shear flow occurs, the drag coefficient is the same as the friction coefficient, that is,

$$c_D = 0.00051.$$

This is significantly smaller than the case of a free boundary layer described above ($c_D = 0.0015$).

Note that for turbulent flow c_D changes only slightly as the plate separation decreases; for example, $c_D = 0.00056$ at half the separation, that is, $H = 0.5$ m.

4.3. Couette flow: with pressure gradient

With a longitudinal pressure gradient present, the shear stress and hence viscous drag beneath the ship will be greater than the zero pressure gradient case described above.

Huey and Williamson (1974) and Lund and Bush (1980) showed experimental and calculated values for c_f up to $\mathrm{Re}_H = 1 \times 10^5$. They found that

$$c_f = 0.004 \text{ at } \mathrm{Re}_H = 1 \times 10^5.$$

Assuming a similar drop in c_f as for flow in a pipe (50% decrease from $\mathrm{Re}_H = 1 \times 10^5$ to 5×10^6), we would expect that

$$c_f \approx 0.002 \text{ at } \mathrm{Re}_H = 5 \times 10^6.$$

As discussed earlier, the mean flow speed beneath the ship will not be as large as the ship speed, and hence this is an overestimate for c_f. A more accurate estimate for c_f may be obtained by finding the value for a boundary layer of the same thickness as the underkeel clearance. This will have a similar velocity distribution and hence c_f as the correct turbulent Couette flow with longitudinal pressure gradient.

Equations (1) and (3) may be combined to express the friction coefficient of a free boundary layer in terms of its thickness δ :

$$c_f = \frac{0.020}{\mathrm{Re}_\delta^{1/6}}$$

$$\mathrm{Re}_\delta = \frac{V\delta}{\nu} \qquad (8)$$

For a ship traveling at 10 knots with 1 m of underkeel clearance,

$$\mathrm{Re}_H = 5 \times 10^6$$

A free boundary layer of this same thickness (1 m) would have

$$\mathrm{Re}_\delta = 5 \times 10^6$$

and, hence, from equation (8),

$$c_f = 0.0015.$$

We see that this estimate of the friction coefficient for flow beneath the ship at small underkeel clearance is similar to the frictional drag coefficient for a ship at large underkeel clearance ($c_D = 0.0015$).

The ship at large underkeel clearance will have a large friction coefficient at the bow, and small friction coefficient at the stern. The ship at small underkeel clearance will have a similar friction coefficient over the whole flat bottom of the hull.

Therefore, the frictional drag coefficient for flow beneath the ship is *not* expected to change significantly as the underkeel clearance becomes small. The only resistance increase in shallow water should be due to shallow water flow effects (as described in Schlichting 1934), with no explicit dependence on underkeel clearance.

5. Effect of small underkeel clearance on squat

Another important reason for studying the flow beneath ships operating at small underkeel clearance is to gauge the effect on squat. Will the modified flow beneath the ship increase or decrease the squat at small underkeel clearance?

5.1. Slender-body shallow-water theory

Squat prediction methods based on slender-body theory (Tuck 1966, Gourlay 2000) have no explicit dependence on underkeel clearance. From linear slender-body shallow-water theory (Tuck 1966) the sinkage and trim of a vessel should be given by

$$s_{\mathrm{LCF}} = c_s\frac{\nabla}{L_{\mathrm{PP}}^2}\frac{F_h^2}{\sqrt{1 - F_h^2}} \qquad (9)$$

$$\theta = c_\theta\frac{\nabla}{L_{\mathrm{PP}}^2}\frac{F_h^2}{\sqrt{1 - F_h^2}} \qquad (10)$$

where

s_{LCF} = sinkage at the longitudinal center of floatation (m) due
to squat

θ = bow-down change in trim (m) due to squat, that is, dif-
ference between sinkage at fore and aft posts

L_{pp} = length between perpendiculars (m)

∇ = displaced volume (m^3)

$F_h = \dfrac{V}{\sqrt{gh}}$ = depth-based Froude number

V = ship speed (m/s)

g = acceleration due to gravity = 9.81 m/s^2

h = water depth (m)

c_s = sinkage coefficient

c_θ = trim coefficient.

According to this theory, the nondimensional coefficients c_s, c_θ depend only on the ship geometry and can be calculated numerically for a given ship. Several semiempirical methods (Hooft 1974, Huuska 1976, Millward 1992) are based on the same formulations, (9) and (10), but use coefficients derived from model tests rather than calculated according to slender-body shallow-water theory.

Like the resistance formulations of Schlichting (1934), the formulations (9) and (10) depend on the section area distribution of the ship and the water depth but have no explicit dependence on underkeel clearance.

5.2. Comparison with lubrication theory

We have already seen that the turbulent Couette flow beneath a ship at small underkeel clearance is likely to have a small near-constant longitudinal pressure gradient.

However, there is the potential for further effects on the pressure beneath the hull in regions where the underkeel clearance is changing (i.e., at the bow and stern).

For example, a low Reynolds number counterpart of the flow beneath a ship at small underkeel clearance is the flow of oil in a bearing, where two almost-parallel surfaces, with relative velocity, are separated by a small clearance.

In this case, the flow satisfies Reynolds' equation of hydrodynamic lubrication (see, e.g., Hersey 1966) provided the clearance between the two surfaces is very small, so that pressure changes and flow velocities perpendicular to the surfaces are negligible. Reynolds' equation predicts large pressure changes in such a situation that are capable of supporting large loads in industrial bearings.

The pressure changes predicted by Reynolds' equation are driven by the changing shear stresses in the flow, whereas inviscid pressure changes predicted by Bernoulli's equation are driven by inertial effects.

Because the Reynolds numbers for flow beneath a ship are so high, lubrication-type pressures as predicted by Reynolds' equation will not be experienced for flow beneath a ship. Also, any such pressures will be diluted by the finite lateral extent of the ship.

Therefore, we may expect that even in the presence of a viscous shear layer beneath a ship at small underkeel clearance, hull pressure and hence squat should be well predicted by inviscid theory.

5.3. Some small underkeel clearance experimental results

We shall reproduce here some experimental squat results obtained by Limpus (2002) at the Australian Maritime College. This set of experiments used a MarAd L-Series model (Roseman 1987) with the following particulars:

L_{pp} = 1.698 m
Beam = 0.340 m
Draft = 0.077 m
Displacement = 36.4 kg
Waterplane area, A_W = 0.548 m^2.
Second moment of waterplane area about the longitudinal center of floatation, I_{LCF} = 0.1187 m^4.

Vertical force Z and pitching moment M were measured rather than actual sinkage and trim. These can be inferred based on hydrostatic balancing:

$$Z = \rho g A_W s_{LCF} \tag{11}$$

$$M = \frac{\rho g I_{LCF}\theta}{L_{PP}} \tag{12}$$

Combining equations (9) through (12) allows us to find the experimentally determined coefficients c_s, c_θ using the experimental values of Z and M, that is,

$$c_s = \frac{Z}{\rho g A_W}\frac{L_{PP}^2}{\nabla}\frac{\sqrt{1 - F_h^2}}{F_h^2} \tag{13}$$

$$c_\theta = \frac{M}{\rho g I_{LCF}}\frac{L_{PP}^2}{\nabla}\frac{\sqrt{1 - F_h^2}}{F_h^2} \tag{14}$$

The experimentally determined sinkage coefficient c_s is plotted in Fig. 4 for varying depth/draft (h/T) ratios. The predicted value according to shallow-water slender-body theory, which is constant, is also plotted. The Froude number range is chosen to represent realistic ship speeds in each depth of water.

The possible error in sinkage and trim coefficients is estimated at around 10% for these tests. Accurate error analyses are difficult, due to such factors as tank seiching and carriage vibration, which are difficult to quantify. We can see from Fig. 4 that the sinkage coefficient stays approximately constant (within 10% to 15%) when h/T becomes small, with no clear trend. This shows that there is no major effect on sinkage at very small underkeel clearance.

Incidentally, these experimental results confirm the use of the sinkage coefficient method for estimating sinkage, in that the measured values of the sinkage coefficient are approximately constant over the complete range of water depths and ship speeds. The theoretical value of the sinkage coefficient slightly underpredicts the experimental results, which is thought to be partly due to the omission of nonlinear terms in the analysis.

The experimental trim coefficient c_θ is plotted in Fig. 5 for varying depth/draft (h/T) ratios, along with the predicted value according to shallow-water slender-body theory.

Again, there is no clear difference between the results at different depth/draft ratios, showing that a small underkeel clearance does not have a significant effect on vessel trim, other than through the normal shallow-water effect.

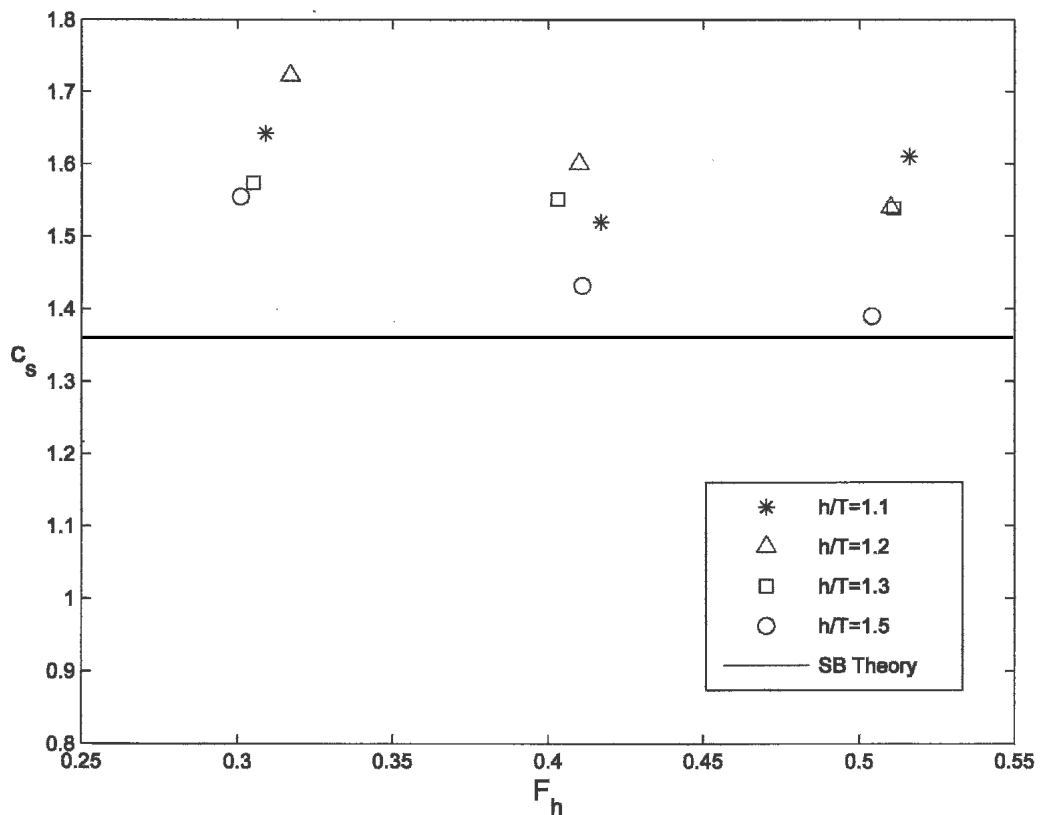As an aside, we notice that the experimental trim coefficient is

Fig. 4 LCF sinkage coefficient c_s as a function of depth Froude number F_h, for different depth/draft (h/T) ratios
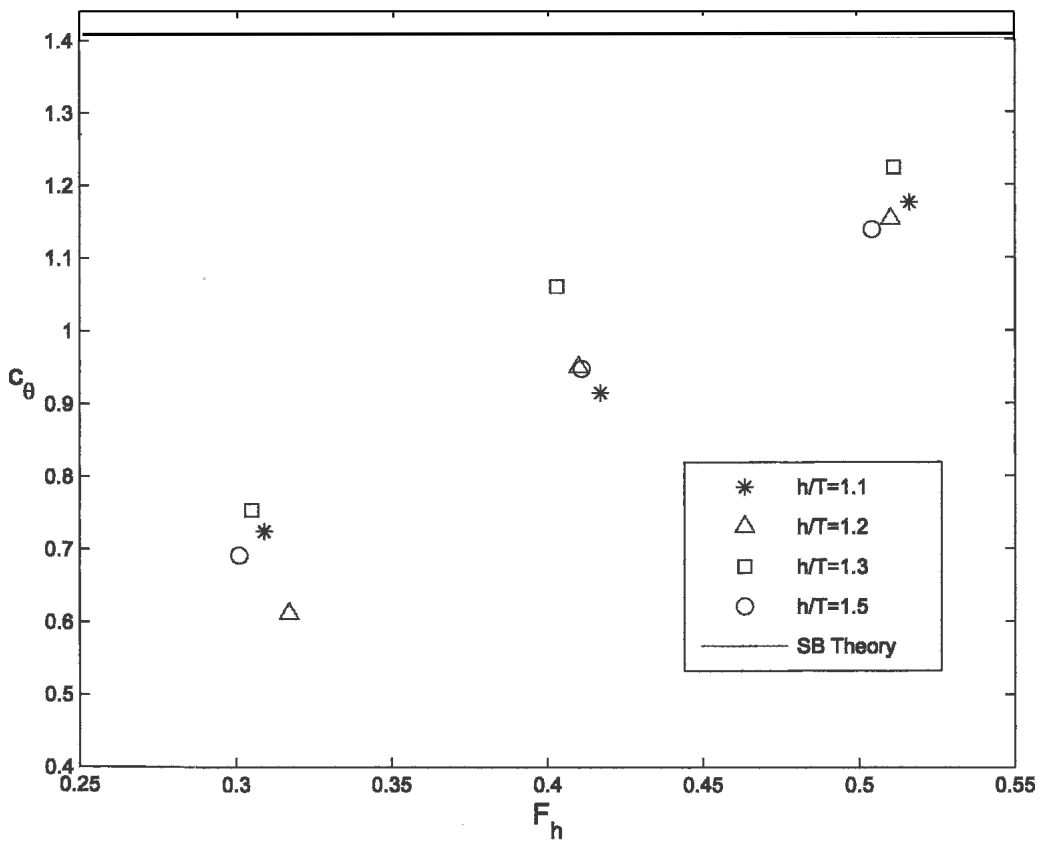

Fig. 5 Trim coefficient c_θ as a function of depth Froude number F_h, for different depth/draft (h/T) ratios
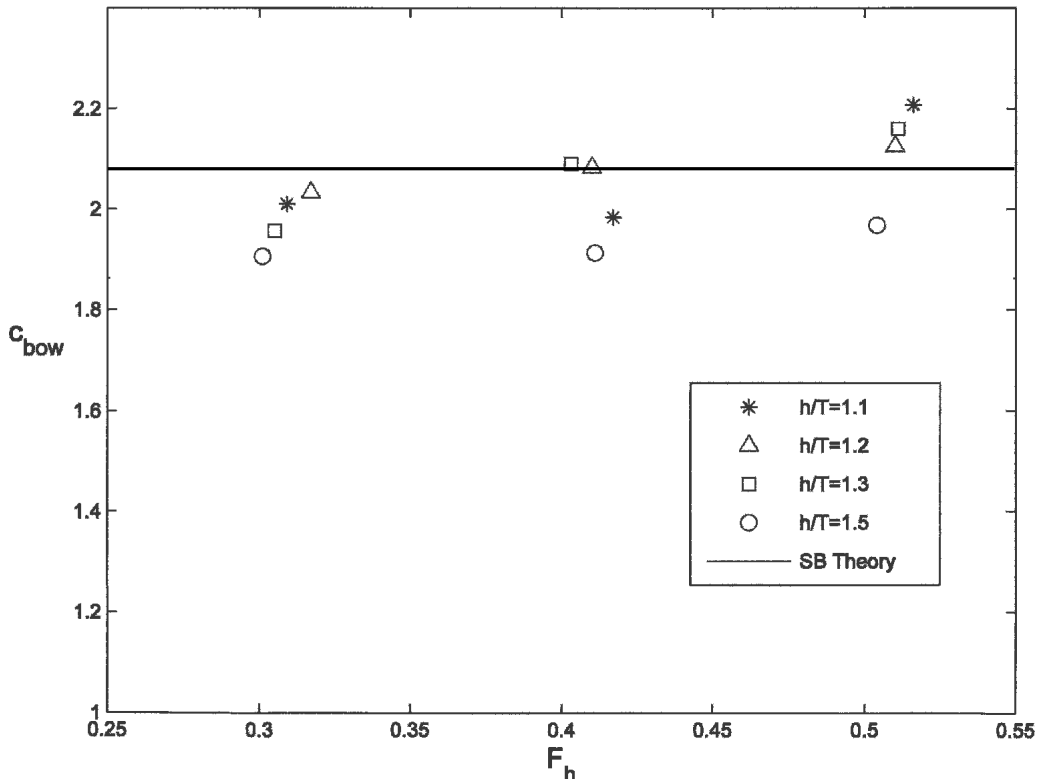
Fig. 6 Bow sinkage coefficient c_{bow} as a function of depth Froude number F_h, for different depth/draft (h/T) ratios

generally overpredicted by the theory. It also shows appreciable variation with depth Froude number, meaning that such a formulation is not as appropriate for trim as for sinkage. These effects are partly due to the viscous effect of flow separation at the stern, which has a significant impact on the trim.

The bow sinkage at the forward post S_{bow} is of particular interest for full-form vessels, which tend to trim by the head. The bow sinkage is calculated using the LCF sinkage and trim. We can nondimensionalize the bow sinkage in the same way as the LCF sinkage, that is,

$$s_{\text{bow}} = c_{\text{bow}} \frac{\nabla}{L_{\text{PP}}^2} \frac{F_h^2}{\sqrt{1 - F_h^2}} \qquad (15)$$

Bow sinkage is shown in Fig. 6. Interestingly, the tendency of the theory to underpredict the LCF sinkage, and overpredict the bow-down trim, means that the prediction of *bow* sinkage (which is of most interest for full-form vessels) is actually quite good.

6. Conclusions

The flow beneath a ship operating at small underkeel clearance can be described by Couette flow, which is the flow between two plates, one of which is moving.

This Couette flow will be turbulent at full scale but may be laminar at model scale. The flow will be affected by longitudinal pressure gradient, so that the velocity distribution will lie somewhere between an antisymmetric distribution and a zero net flow distribution.

The implication of this flow model on viscous resistance is that frictional drag on the bottom of the hull is expected to remain approximately *constant* when the underkeel clearance becomes very small. Therefore, the resistance increase of a ship in shallow water should be adequately described by the changed wave pattern and larger flow speeds around the sides of the ship, without any explicit underkeel clearance effect.

The effect of a turbulent shear flow on the hydrodynamic pressures beneath the hull has also been analyzed. It is shown that for practical underkeel clearances any shear-induced pressure increase beneath the hull is expected to be very small. Therefore, there should be no noticeable effect on ship squat at small underkeel clearance, beyond the normal increase due to shallow-water effect. This was demonstrated with reference to a comparison between slender-body shallow-water theory and experimental results.

Acknowledgment

References

BECK, R. F., AND TUCK, E. O. 1972 Computation of shallow water ship motions. *Proceedings,* 9th Symposium on Naval Hydrodynamics, August, Paris.

CHEN, X.-N., AND SHARMA, S. D. 1995 A slender ship moving at a near-critical speed in a shallow channel, *Journal of Fluid Mechanics,* **291,** 263.

GOURLAY, T. P., AND TUCK, E. O. 2001 The maximum sinkage of a ship, JOURNAL OF SHIP RESEARCH, **45,** 1, 50.

GOURLAY, T. P. 2000 *Mathematical and Computational Techniques for Predicting the Squat of Ships,* Ph.D. thesis, University of Adelaide.

HARVALD, SV.AA. 1983 *Resistance and Propulsion of Ships,* Wiley-Interscience, New York.

HERSEY, M. D. 1966 *Theory and Research in Lubrication,* John Wiley & Sons, New York.

HOOFT, J. P. 1974 The behaviour of a ship in head waves at restricted water depth, *International Shipbuilding Progress,* **244,** 21, 367.

HUEY, L. J., AND WILLIAMSON, J. W. 1974 Plane turbulent Couette flow with zero net flow, *Journal of Applied Mechanics,* **41,** 885.

HUUSKA, O. 1976 *On the Evaluation of Underkeel Clearances in Finnish Waterways,* Helsinki University of Technology Ship Hydrodynamics Laboratory, Otaniemi, Report no. 9.

LIMPUS, W. 2002 *The Effect of Low Underkeel Clearances on Squat,* B. Naval Architecture thesis, Australian Maritime College.

LUND, K. O., AND BUSH, W. B. 1980 Asymtotic analysis of plane turbulent Couette-Poiseuille flows, *Journal of Fluid Mechanics,* **96,** 81.

MEI, C. C. 1976 Flow around a thin body moving in shallow water, *Journal of Fluid Mechanics,* **77,** 737.

MILLWARD, A. 1992 A comparison of the theoretical and empirical prediction of squat in shallow water. *International Shipbuilding Progress,* **417,** 39, 69.

PRANDTL, L. 1904 Über Flüssigkeitsbewegung bei sehr kleiner Reibung, *Proceedings,* 3rd International Mathematics Congress, Heidelberg, Germany.

REICHARDT, H. 1956 Über die Geschwindigkeitsverteilung in einer geradlinigen turbulenten Couette-Strömung, *Zeit. Angew. Math. Mech.,* **36,** Sonderheft (special issue), 26.

ROSEMAN, D. P., editor. 1987 *The MarAd Systematic Series of Full Form Ship Models,* Society of Naval Architects and Marine Engineers, Jersey City, NJ.

SCHLICHTING, H. 1968 *Boundary-Layer Theory,* 6th ed., McGraw-Hill, New York.

SCHLICHTING, O. 1934 Schiffwiderstand auf beschränkter Wassertiefe: Widerstand von Seeschiffen auf flachem Wasser, *Jahrbuch der Schiffbautechnischen Gesellschaft,* **35,** 127.

TUCK, E. O. 1966 Shallow water flows past slender bodies, *Journal of Fluid Mechanics,* **26,** 81.

WHITE, F. M. 1999 *Fluid Mechanics,* 4th ed., McGraw-Hill, New York.